

# On an integral equation arising in the transport of radiation through a slab involving internal reflection

## II. Generalisation and numerical results for the Fresnel case

M.M.R. Williams<sup>a,b</sup>

Computational Physics and Geophysics, Department of Earth Science and Engineering, Imperial College of Science, Technology and Engineering, Prince Consort Road, London, SW7 2BP, UK

Received 12 July 2006

Published online 6 October 2006 – © EDP Sciences, Società Italiana di Fisica, Springer-Verlag 2006

**Abstract.** In an earlier contribution to this journal [M.M.R. Williams, Eur. Phys. J. B **47**, 291 (2005)], we derived an integral equation for the transmission of radiation through a slab of finite thickness which incorporated internal reflection at the surfaces. Here we generalise the problem to the case when there is a source on each face and the reflection coefficients are different at each face. We also discuss numerical and analytic solutions of the equation discussed in [M.M.R. Williams, Eur. Phys. J. B **47**, 291 (2005)] when the reflection is governed by the Fresnel conditions. We obtain numerical and graphical results for the reflection and transmission coefficients, the scalar intensity and current and the emergent angular distributions at each face. The incident source is either a mono-directional beam or a smoothly varying distribution which goes from isotropic to a normal beam. Of particular interest is the philosophy of the numerical solution and whether a direct numerical approach is more effective than one involving a more elegant analytical solution using replication and the Hilbert problem. We also develop the solution of this problem using diffusion theory and compare the results with the exact transport solution.

**PACS.** 05.60.Cd Classical transport

## 1 Introduction

The transmission of radiation through turbid media has been of considerable interest for many years. It is assuming even more importance now because of the development of tissue scanning devices which employ infra-red radiation. The interpretation of the scans requires ever more sophisticated models and mathematical procedures. In our earlier work [1], we have derived an integral equation for the scalar intensity of radiation and its associated angular distribution. It is the purpose of the present work to show how an analytical solution to that equation may be obtained and to compare the practical aspects of solving the analytical equations with that of a direct numerical assault on the original equation. Accurate results are obtained for a range of physical parameters and these are compared with those arising from diffusion theory. In addition, for more generality, we have derived the equations necessary to deal with the case when there is a source incident on each face of the slab and each face has a different Fresnel coefficient.

To clarify further some practical implications of this work, we refer the reader to work done by Nieuwenhuizen and Luck [2] and a more extensive review by van Rossum and Nieuwenhuizen [3]. These works concentrate on the skin layer in the neighbourhood of the slab boundary where diffusion theory breaks down. Methods are developed based upon the ‘thick slab’ problem, where the interaction between the boundaries is neglected. A number of results which modify the diffusion theory boundary conditions are developed and enable diffusion theory to be used with greater accuracy. The present work, whilst not analytically based, extends the validity of that approach. Reference [3] in particular extends the work to non-planar problems and enables the effects of local inhomogeneities, such as spheres embedded in slabs, to be studied by the concept of the dipole moment. Reference [4] by Luck and Nieuwenhuizen, further develops the diffusion approach and treats inhomogeneities by multipole expansions, with appropriate modifications using transport corrections when the inhomogeneities are small compared with a mean free path. Finally, we note a very interesting application of one-dimensional transport theory to the study of the visual effects of art glazes as arising in the study of ‘old masters’ [5]. Applications of the theory can

---

<sup>a</sup> All correspondence to 2a Lytchgate Close, South Croydon, Surrey, CR2 0DX, UK.

<sup>b</sup> e-mail: [mmrw@nuclear-energy.demon.co.uk](mailto:mmrw@nuclear-energy.demon.co.uk)

lead to the discovery of the nature of the pigmentation embedded in the oil binder. Of course, our present work does not refer directly to these practical problems but it does provide a measure of their accuracy.

## 2 Theory

We may write the equation of radiative transfer for the angular photon intensity  $\phi(\tau, \mu)$  for isotropic scattering as [6],

$$\mu \frac{\partial \phi(\tau, \mu)}{\partial \tau} + \phi(\tau, \mu) = \frac{c}{2} \int_{-1}^1 d\mu' \phi(\tau, \mu') \equiv \frac{c}{2} \phi_0(\tau) \quad (1)$$

where  $c = \Sigma_s / (\Sigma_s + \Sigma_a)$ . The scattering cross section is defined by  $\Sigma_s$  and the absorption cross section by  $\Sigma_a$ . We have tacitly assumed isotropic scattering but by means of the transport approximation [6], the above theory still applies provided we make the following replacements:

$$\tau \rightarrow x [\Sigma_s (1 - \bar{\mu}_0) + \Sigma_a], \quad c \rightarrow \frac{\Sigma_s (1 - \bar{\mu}_0)}{\Sigma_s (1 - \bar{\mu}_0) + \Sigma_a} \quad (2)$$

where  $\bar{\mu}_0$  is the mean cosine of scattering of a photon.

The boundary conditions associated with equation (1) which describe internal reflection are

$$\phi(0, \mu) = R_1(\mu) \phi(0, -\mu) + q_1(\mu); \quad \mu > 0 \quad (3a)$$

$$\phi(a, \mu) = R_2(-\mu) \phi(a, -\mu) + q_2(-\mu); \quad \mu < 0 \quad (3b)$$

with  $R_1(\mu)$  the reflection coefficient and  $q_1(\mu)$  the incident distribution at  $\tau = 0$  and  $R_2(\mu)$  and  $q_2(\mu)$  for the face at  $\tau = a$ . Following the method used in [1], equation (1) may be integrated and, together with the boundary conditions, leads to (for  $\mu > 0$ )

$$\begin{aligned} \phi(a, \mu) = & \frac{1}{1 - R_1(\mu)R_2(\mu)e^{-2a/\mu}} \\ & \times \left[ q_1(\mu) e^{-a/\mu} + q_2(\mu) R_1(\mu) e^{-2a/\mu} \right. \\ & \left. + \frac{c}{2\mu} \int_0^a d\tau' \phi_0(\tau') \left( R_1(\mu) e^{-(a+\tau')/\mu} + e^{-(a-\tau')/\mu} \right) \right] \end{aligned} \quad (4a)$$

$$\begin{aligned} \phi(0, -\mu) = & \frac{1}{1 - R_1(\mu)R_2(\mu)e^{-2a/\mu}} \\ & \times \left[ q_2(\mu) e^{-a/\mu} + q_1(\mu) R_2(\mu) e^{-2a/\mu} \right. \\ & \left. + \frac{c}{2\mu} \int_0^a d\tau' \phi_0(\tau') \left( e^{-\tau'/\mu} + R_2(\mu) e^{-(2a-\tau')/\mu} \right) \right] \end{aligned} \quad (4b)$$

and the following integral equation for the scalar intensity  $\phi_0(\tau)$ ,

$$\begin{aligned} \phi_0(\tau) = & \int_0^1 \frac{d\mu f(\mu)}{1 - R_1(\mu)R_2(\mu)e^{-2a/\mu}} \\ & + \frac{c}{2} \int_0^a d\tau' \phi_0(\tau') (E_1(|\tau - \tau'|) + K(\tau, \tau')) \end{aligned} \quad (5)$$

where

$$\begin{aligned} f(\mu) = & q_1(\mu) \left( e^{-\tau/\mu} + R_2(\mu) e^{-(2a-\tau)/\mu} \right) \\ & + q_2(\mu) \left( e^{-(a-\tau)/\mu} + R_1(\mu) e^{-(a+\tau)/\mu} \right) \end{aligned}$$

and

$$K(\tau, \tau') = \int_0^1 \frac{d\mu g(\mu)}{\mu (1 - R_1(\mu)R_2(\mu)e^{-2a/\mu})}$$

with

$$\begin{aligned} g(\mu) = & R_1(\mu) e^{-(\tau+\tau')/\mu} + R_2(\mu) e^{-(2a-\tau-\tau')/\mu} \\ & + R_1(\mu) R_2(\mu) \left( e^{-(2a+\tau-\tau')/\mu} + e^{-(2a-\tau+\tau')/\mu} \right). \end{aligned} \quad (6)$$

In many practical cases, it is the surface angular distributions  $\phi(0, -\mu)$  and  $\phi(a, \mu)$  which are of interest. These can be obtained from a solution of equation (5) and insertion into (4a,b). It is the solution of equation (5) and the associated angular distributions which form the purpose of this work. First however we note that one can define the radiation current  $J(\tau)$  as

$$J(\tau) = \int_{-1}^1 d\mu \mu \phi(\tau, \mu) \quad (7)$$

where using (4a,b) we find

$$\begin{aligned} J(\tau) = & \int_0^1 \frac{d\mu \mu h(\mu)}{1 - R_1(\mu)R_2(\mu)e^{-2a/\mu}} \\ & + \frac{c}{2} \int_0^a d\tau' \phi_0(\tau') (\text{sgn}(\tau - \tau') E_2(|\tau - \tau'|) + N(\tau, \tau')) \end{aligned} \quad (8)$$

with

$$\begin{aligned} h(\mu) = & q_1(\mu) \left( e^{-\tau/\mu} - R_2(\mu) e^{-(2a-\tau)/\mu} \right) \\ & - q_2(\mu) \left( e^{-(a-\tau)/\mu} - R_1(\mu) e^{-(a+\tau)/\mu} \right) \end{aligned}$$

and

$$N(\tau, \tau') = \int_0^1 \frac{d\mu k(\mu)}{(1 - R_1(\mu)R_2(\mu)e^{-2a/\mu})}$$

with

$$k(\mu) = R_1(\mu)e^{-(\tau+\tau')/\mu} - R_2(\mu)e^{-(2a-\tau-\tau')/\mu} + R_1(\mu)R_2(\mu)\left(e^{-(2a+\tau-\tau')/\mu} - e^{-(2a-\tau+\tau')/\mu}\right). \quad (9)$$

The form for the reflection coefficient is that due to Fresnel [7] and can be written

$$R_i(\mu) = \frac{1}{2} \left[ \left( \frac{\mu - n_i \sqrt{1 - n_i^2(1 - \mu^2)}}{\mu + n_i \sqrt{1 - n_i^2(1 - \mu^2)}} \right)^2 + \left( \frac{n_i \mu - \sqrt{1 - n_i^2(1 - \mu^2)}}{n_i \mu + \sqrt{1 - n_i^2(1 - \mu^2)}} \right)^2 \right]; \quad \mu_{ci} < \mu < 1$$

$$= 1; \quad 0 < \mu < \mu_{ci} \quad (10)$$

$$\tilde{R}_i(\mu) = \frac{1}{2} \left[ \left( \frac{n_i^2 \mu - \sqrt{n_i^2 - 1 + \mu^2}}{n_i^2 \mu + \sqrt{n_i^2 - 1 + \mu^2}} \right)^2 + \left( \frac{\mu - \sqrt{n_i^2 - 1 + \mu^2}}{\mu + \sqrt{n_i^2 - 1 + \mu^2}} \right)^2 \right]; \quad 0 < \mu < 1 \quad (11)$$

$$\tilde{R}_i\left(\sqrt{1 - n_i^2(1 - \mu^2)}\right) = R_i(\mu); \quad \mu_{ci} < \mu < 1 \quad (12)$$

$$R_i\left(\sqrt{1 - (1 - \mu^2)/n_i^2}\right) = \tilde{R}_i(\mu) \quad (13)$$

where  $\mu_{ci} = (1 - 1/n_i^2)^{1/2}$ . We also note that  $R_i(\mu)$  is the Fresnel coefficient for the case when radiation passes from an optically dense to an optically less dense medium, and  $\tilde{R}_i(\mu)$  is the reverse situation.

The source term  $q_i(\mu)$  in equations (3a) and (3b) needs some explanation. This corresponds to the radiation from the incident source  $\psi_i(\mu)$  which has been transmitted through the surface. Thus we can write it as

$$q_i(\mu) = n_i^2(1 - R_i(\mu))\psi_i\left(\sqrt{1 - n_i^2(1 - \mu^2)}\right) \times \Theta(\mu_{ci} < \mu < 1) \quad (14)$$

which accounts for refraction at the surface via Snell's law [7].  $\Theta(a < \mu < b)$  is equal to unity if  $a < \mu < b$  and zero otherwise. In addition to the above quantities, we need the emergent angular distributions from faces  $\tau = 0$  and  $a$ . Namely,

$$\phi_{out}(0, -\mu_t) = \tilde{R}_1(\mu_t)\psi_1(\mu_t) + \frac{1}{n_1^2}(1 - R_1(\mu))\phi(0, -\mu) \quad (15)$$

$$\phi_{out}(a, \mu_t) = \tilde{R}_2(\mu_t)\psi_2(\mu_t) + \frac{1}{n_2^2}(1 - R_2(\mu))\phi(a, \mu) \quad (16)$$

where  $\mu_t = \sqrt{1 - n^2(1 - \mu^2)}$  with  $\mu_c < \mu < 1$  and  $0 < \mu_t < 1$ . The presence of  $n^2$  and  $1/n^2$  in the above equations accounts for the solid angle effect associated with the limited range due to  $\mu_c$  [8,14].

There are two integral parameters of considerable importance, namely the reflection coefficient  $R_s$  and transmission coefficient  $T_s$ . These are defined at the face  $\tau = 0$  by

$$R_s(0) = \left[ \int_{\mu_{c1}}^1 d\mu \mu (1 - R_1(\mu))\phi(0, -\mu) + \int_0^1 d\mu \mu \tilde{R}_1(\mu)\psi_1(\mu) \right] / \int_0^1 d\mu \mu \psi_1(\mu) \quad (17a)$$

where the second term is the contribution from direct surface reflection. If  $\psi_1 = 0$ , this becomes a transmission coefficient related to the source at  $\tau = a$ , whence

$$T_s(0) = \int_{\mu_{c1}}^1 d\mu \mu (1 - R_1(\mu))\phi(0, -\mu) / \int_0^1 d\mu \mu \psi_2(\mu) \quad (17b)$$

By analogy, for the face at  $\tau = a$ ,

$$R_s(a) = \left[ \int_{\mu_{c2}}^1 d\mu \mu (1 - R_2(\mu))\phi(a, \mu) + \int_0^1 d\mu \mu \tilde{R}_2(\mu)\psi_2(\mu) \right] / \int_0^1 d\mu \mu \psi_2(\mu) \quad (18a)$$

and

$$T_s(a) = \int_{\mu_{c2}}^1 d\mu \mu (1 - R_2(\mu))\phi(a, \mu) / \int_0^1 d\mu \mu \psi_1(\mu) \quad (18b)$$

But it may also be shown from these definitions and the boundary conditions that

$$R_s(0) = \int_0^1 d\mu \mu \psi_1(\mu) - J(0), \quad R_s(a) = \int_0^1 d\mu \mu \psi_2(\mu) + J(a) \quad (19)$$

which are easier to evaluate numerically than (17) and (18).

### 3 Analytical solution of the integral equation

For the purposes of example in this paper, we assume that  $R_1 = R_2 = R$ ,  $q_2 = 0$  and  $q_1 = q$ . Thus the integral equation (5) simplifies to the one derived in [1]. While

equation (5) is open to a numerical solution, and indeed we will return to this matter below, it is useful to see what analytical results can be deduced. To do this we use the method of replication [9], in which we seek a solution to the integral equation in the following form

$$\phi_0(\tau) = A_0 e^{-\nu\tau} + B_0 e^{\nu\tau} + \int_0^1 d\omega \left[ A(\omega) e^{-\tau/\omega} + B(\omega) e^{\tau\omega} \right] \quad (20)$$

Inserting this expression into equation (5) and collecting up coefficients of  $e^{\pm\nu\tau}$  and  $e^{\pm\tau/\mu}$ , we find the following results.

From  $e^{\pm\nu\tau}$ , we find that  $\nu$  must satisfy the transcendental equation

$$1 = \frac{c}{2\nu} \log \left( \frac{1+\nu}{1-\nu} \right) \quad (21)$$

and  $A(\omega)$  and  $\tilde{B}(\omega) = e^{a/\omega} B(\omega)$ , satisfy the following singular integral equations,

$$\begin{aligned} A(\omega) A(\omega) + \frac{c}{2} \int_0^1 \frac{d\mu \mu A(\mu)}{\mu - \omega} = & \\ \omega \Delta(\omega) \frac{c}{2} \int_0^1 d\mu A(\mu) \left\{ \frac{\mu}{\omega + \mu} \left( 1 - e^{-(1/\mu+1/\omega)a} \right) \right. & \\ \left. + \frac{\mu R(\omega)}{\mu - \omega} \left( e^{-a/\mu} - e^{-a/\omega} \right) e^{-a/\omega} \right\} & \\ - \frac{c}{2} \int_0^1 d\mu \tilde{B}(\mu) \left[ \frac{\mu e^{-a/\mu}}{\omega + \mu} - \omega \Delta(\omega) \right. & \\ \times \left\{ \frac{\mu}{\mu - \omega} \left( e^{-a/\mu} - e^{-a/\omega} \right) \right. & \\ \left. + \frac{\mu R(\omega)}{\mu + \omega} \left( 1 - e^{-(1/\mu+1/\omega)a} \right) e^{-a/\omega} \right\} & \\ - \frac{c}{2} A_0 \left[ \frac{1}{1 - \nu\omega} - \omega \Delta(\omega) \right] \left\{ \frac{1}{1 + \nu\omega} \left( 1 - e^{-(\nu+1/\omega)a} \right) \right. & \\ \left. + \frac{R(\omega)}{1 - \nu\omega} \left( e^{-\nu a} - e^{-a/\omega} \right) e^{-a/\omega} \right\} & \\ - \frac{c}{2} B_0 \left[ \frac{1}{1 + \nu\omega} - \omega \Delta(\omega) \right] \left\{ \frac{1}{1 - \nu\omega} \left( 1 - e^{-(1/\omega-\nu)a} \right) \right. & \\ \left. + \frac{R(\omega)}{1 + \nu\omega} \left( e^{\nu a} - e^{-a/\omega} \right) e^{-a/\omega} \right\} & \\ + \frac{q(\omega)}{1 - R^2(\omega) e^{-2a/\omega}} & \end{aligned} \quad (22)$$

and

$$\begin{aligned} A(\omega) \tilde{B}(\omega) + \frac{c}{2} \int_0^1 \frac{d\mu \mu \tilde{B}(\mu)}{\mu - \omega} = & \\ \omega \Delta(\omega) \frac{c}{2} \int_0^1 d\mu \tilde{B}(\mu) \left\{ \frac{\mu}{\omega + \mu} \left( 1 - e^{-(1/\mu+1/\omega)a} \right) \right. & \\ \left. + \frac{\mu R(\omega)}{\mu - \omega} \left( e^{-a/\mu} - e^{-a/\omega} \right) e^{-a/\omega} \right\} & \\ - \frac{c}{2} \int_0^1 d\mu A(\mu) \left[ \frac{\mu e^{-a/\mu}}{\omega + \mu} - \omega \Delta(\omega) \right. & \\ \times \left\{ \frac{\mu}{\mu - \omega} \left( e^{-a/\mu} - e^{-a/\omega} \right) \right. & \\ \left. + \frac{\mu R(\omega)}{\mu + \omega} \left( 1 - e^{-(1/\mu+1/\omega)a} \right) e^{-a/\omega} \right\} & \\ - \frac{c}{2} A_0 \left[ \frac{e^{-\nu a}}{1 + \nu\omega} - \omega \Delta(\omega) \right] \left\{ \frac{1}{1 - \nu\omega} \left( e^{-\nu a} - e^{-a/\omega} \right) \right. & \\ \left. + \frac{R(\omega)}{1 + \nu\omega} \left( 1 - e^{-(\nu+1/\omega)a} \right) e^{-a/\omega} \right\} & \\ - \frac{c}{2} B_0 \left[ \frac{e^{\nu a}}{1 - \nu\omega} - \omega \Delta(\omega) \right] \left\{ \frac{1}{1 + \nu\omega} \left( e^{\nu a} - e^{-a/\omega} \right) \right. & \\ \left. + \frac{R(\omega)}{1 - \nu\omega} \left( 1 - e^{-(1/\omega-\nu)a} \right) e^{-a/\omega} \right\} & \\ + \frac{q(\omega) R(\omega) e^{-a/\omega}}{1 - R^2(\omega) e^{-2a/\omega}} & \end{aligned} \quad (23)$$

where  $\Delta(\omega)$  is defined by equation (46) and

$$A(\omega) = 1 - \frac{c\omega}{2} \log \left( \frac{1+\omega}{1-\omega} \right).$$

Equations (22) and (23) are a pair of coupled singular integral equations. The right hand sides contain two unknown constants  $A_0$  and  $B_0$ . In order to define these it is necessary to note that the adjoint solution of the homogeneous equation must be orthogonal to the right hand sides of (22) and (23). Now if we write for convenience equations (22) and (23) [15] as

$$A(\omega) A(\omega) + \frac{c}{2} \int_0^1 \frac{d\mu \mu A(\mu)}{\mu - \omega} = f(\omega) \quad (24)$$

and

$$A(\omega) \tilde{B}(\omega) + \frac{c}{2} \int_0^1 \frac{d\mu \mu \tilde{B}(\mu)}{\mu - \omega} = g(\omega) \quad (25)$$

then the adjoint solution  $A^\dagger(\omega)$  of the left hand side of equation (24) is given by

$$A(\omega) A^\dagger(\omega) + \frac{c}{2} \int_0^1 \frac{d\mu \mu A^\dagger(\mu)}{\omega - \mu} = 0 \quad (26)$$

It is readily shown [15] that a solution to equation (24) can only exist if

$$\int_0^1 d\omega A^\dagger(\omega) f(\omega) = 0 \quad (27)$$

and a solution to equation (25) if

$$\int_0^1 d\omega \tilde{B}^\dagger(\omega) g(\omega) = 0. \quad (28)$$

These equations provide the necessary conditions to solve for  $A_0$  and  $B_0$ . Using the methods of complex variables, we can show that

$$A^\dagger(\omega) = \tilde{B}^\dagger(\omega) = \frac{c\nu}{2\sqrt{1-c}} \frac{\omega H(\omega)}{1-\nu\omega} \quad (29)$$

where  $H(\omega)$  is Chandrasekhar's  $H$ -function [9].

There are now three ways to proceed to solve the coupled integral equations. The first is to continue with the method of complex variables [9], in which case we can reduce the singular integral equations (22) and (23) to a pair of coupled non-singular integral equations involving  $H$  functions and related quantities. This then requires extensive numerical work to find  $A(\omega)$  and  $\tilde{B}(\omega)$ . A practical alternative is to use the FN method [10,11] which essentially solves numerically the singular integral equations directly. Yet another method which we will use here involves quadrature applied directly to equation (5).

## 4 Diffusion theory

It is of some interest to compare the above results with those of diffusion theory as it is much simpler to use. Thus the equation for the scalar flux intensity is [6]

$$\phi_0''(\tau) - \kappa^2 \phi_0(\tau) = 0 \quad (30)$$

where  $\kappa^2 = 3(1-c)$ . The boundary conditions for the Fresnel case, analogous to the simple form of equation (5), can be found in [8,12] and leads to

$$\phi_0(0) - \frac{2\alpha}{3} \phi_0'(0) = \tilde{\psi} \quad (31)$$

$$\phi_0(a) + \frac{2\alpha}{3} \phi_0'(a) = 0 \quad (32)$$

where

$$\alpha = \frac{1 + 3 \int_0^1 d\mu \mu^2 R(\mu)}{1 - 2 \int_0^1 d\mu \mu R(\mu)} \equiv \frac{1 + 3r_2}{1 - 2r_1} \quad (33)$$

and

$$\tilde{\psi} = \frac{4 \int_0^1 d\mu \mu (1 - \tilde{R}(\mu)) \psi(\mu)}{1 - 2 \int_0^1 d\mu \mu R(\mu)} \equiv 4q_0 \quad (34)$$

The solution is readily shown to be

$$\phi_0(\tau) = \frac{4q_0}{D_s} \left[ \left(1 + \frac{2\alpha\kappa}{3}\right) e^{-\kappa\tau} - \left(1 - \frac{2\alpha\kappa}{3}\right) e^{-\kappa(2a-\tau)} \right] \quad (35)$$

where

$$D_s = \left(1 + \frac{2\alpha\kappa}{3}\right)^2 - \left(1 - \frac{2\alpha\kappa}{3}\right)^2 e^{-2\kappa a}.$$

We observe that this solution is similar in form to the asymptotic part of the transport solution of equation (20) where  $\kappa \approx \nu$ .

The current is, following Fick's law, or P1 theory [6],

$$J(\tau) = -\frac{1}{3} \phi_0'(\tau) \quad (36)$$

For a general normalised incident distribution  $\psi(\mu)$ , we have for the reflection and transmission coefficients,

$$R_d = \int_0^1 d\mu \mu \tilde{R}(\mu) \psi(\mu) + \frac{q_0}{D_s} \left[ \left(1 + \frac{2\alpha\kappa}{3}\right) \left(1 - 2r_1 - \frac{2\kappa}{3}(1 - 3r_2)\right) - \left(1 - \frac{2\alpha\kappa}{3}\right) \left(1 - 2r_1 + \frac{2\kappa}{3}(1 - 3r_2)\right) e^{-2\kappa a} \right] \quad (37)$$

and

$$T_d = \frac{8\kappa q_0 e^{-\kappa a}}{3D_s}. \quad (38)$$

For the case of a mono-directional beam,  $\psi(\mu) = \delta(\mu - \mu_0)$ , we have

$$R_{d0} = \tilde{R}(\mu_0) + \frac{\hat{q}_0}{\mu_0 D_s} \left[ \left(1 + \frac{2\alpha\kappa}{3}\right) \left(1 - 2r_1 - \frac{2\kappa}{3}(1 - 3r_2)\right) - \left(1 - \frac{2\alpha\kappa}{3}\right) \left(1 - 2r_1 + \frac{2\kappa}{3}(1 - 3r_2)\right) e^{-2\kappa a} \right] \quad (39)$$

and

$$T_{d0} = \frac{8\kappa \hat{q}_0 e^{-\kappa a}}{3\mu_0 D_s} \quad (40)$$

with

$$\frac{\hat{q}_0}{\mu_0} = \frac{1 - \tilde{R}(\mu_0)}{1 - 2r_1}. \quad (41)$$

It is also useful to observe that  $1 - R - T$  is the fraction of photons absorbed in the slab.

## 5 Numerical solution and discussion

### 5.1 Reduction of the equations to quadratures

Let us write equation (5) in the form

$$\phi_0(\tau) = S(\tau) + \frac{c}{2} \int_0^a d\tau' \phi_0(\tau') M(\tau, \tau'). \quad (42)$$

We now define the average flux in the region  $\Delta\tau = \tau_i - \tau_{i-1}$  or more concisely as

$$\phi_{0i} = \frac{1}{\Delta\tau} \int_{\tau_{i-1}}^{\tau_i} d\tau \phi_0(\tau) \quad (43)$$

and average equation (5) over the range  $\Delta\tau$ , to get

$$\phi_{0i} = S_i + \frac{c}{2\Delta\tau} \sum_{j=1}^N \phi_{0j} M_{ij} \quad ; \quad i = 1, 2, \dots, N \quad (44)$$

where

$$S_i = \frac{1}{\Delta\tau} \int_{\mu_c}^1 d\mu \mu q(\mu) \Delta(\mu) \left[ e^{-\tau_{i-1}/\mu} - e^{-\tau_i/\mu} + R(\mu) \left( e^{-(2a-\tau_i)/\mu} - e^{-(2a-\tau_{i-1})/\mu} \right) \right] \quad (45)$$

and

$$\frac{1}{\Delta(\mu)} = 1 - R(\mu)^2 e^{-2a/\mu}. \quad (46)$$

The matrix element  $M_{ij}$  is defined as

$$M_{ij} = \int_{\tau_{i-1}}^{\tau_i} d\tau \int_{\tau_{i-1}}^{\tau_j} d\tau' M(\tau, \tau') \quad (47)$$

The full expression for this is in Appendix A. Equations (44) are a set of coupled linear algebraic equations for the average fluxes and can be solved by the standard methods of linear algebra. We have used the IMSL Fortran Library routine DLSLSF.

Knowing the  $\phi_{0i}$ , we may use equations (4a,b) to calculate the angular distributions and equations (15) and (16) to obtain the emergent distributions. Thus

$$\begin{aligned} \phi(0, -\mu) &= \Delta(\mu) \\ &\left[ q(\mu) R(\mu) e^{-2a/\mu} + \frac{c}{2} \sum_{i=1}^N \phi_{0i} \left\{ e^{-\tau_{i-1}/\mu} - e^{-\tau_i/\mu} \right. \right. \\ &\left. \left. + R(\mu) \left( e^{-(2a-\tau_i)/\mu} - e^{-(2a-\tau_{i-1})/\mu} \right) \right\} \right] \quad (48) \end{aligned}$$

and

$$\begin{aligned} \phi(a, \mu) &= \Delta(\mu) \\ &\left[ q(\mu) e^{-a/\mu} + \frac{c}{2} \sum_{i=1}^N \phi_{0i} \left\{ e^{-(a-\tau_i)/\mu} - e^{-(a-\tau_{i-1})/\mu} \right. \right. \\ &\left. \left. + R(\mu) \left( e^{-(a+\tau_i)/\mu} - e^{-(a+\tau_{i-1})/\mu} \right) \right\} \right]. \quad (49) \end{aligned}$$

We may also calculate the current  $J(\tau)$  as

$$\begin{aligned} J(\tau) &= \int_0^1 d\mu \mu q(\mu) \frac{e^{-\tau/\mu} - R(\mu) e^{-(2a-\tau)/\mu}}{1 - R^2(\mu) e^{-2a/\mu}} \\ &+ \frac{c}{2} \sum_{j=1}^N \phi_{0j} \int_{\tau_{j-1}}^{\tau_j} d\tau' (\text{sgn}(\tau - \tau') E_2(|\tau - \tau'|) + N(\tau, \tau')) \quad (50) \end{aligned}$$

$$J(\tau) = Q_0(\tau) + \frac{c}{2} \sum_{j=1}^N \phi_{0j} [E_j(\tau) + N_j(\tau)] \quad (51)$$

$E_j$  and  $N_j$  are given in Appendix A.

In the special case of a mono-directional incident beam, we can simplify the equations somewhat as follows. Taking  $\psi(\mu) = \delta(\mu - \mu_0)$ , we have from equation (14) and the properties of the Dirac delta function,

$$\psi\left(\sqrt{1 - n^2(1 - \mu^2)}\right) = \frac{\mu_0}{n^2 \tilde{\mu}_0} \delta(\mu - \tilde{\mu}_0) \quad (52)$$

where

$$\tilde{\mu}_0 = \sqrt{1 - \frac{1 - \mu_0^2}{n^2}}.$$

Thus in (45),

$$\begin{aligned} S_i &= \frac{\mu_0 \left(1 - \tilde{R}(\mu_0)\right)}{1 - \tilde{R}^2(\mu_0) e^{-2a/\tilde{\mu}_0}} \frac{1}{\Delta\tau} \left[ e^{-\tau_{i-1}/\tilde{\mu}_0} - e^{-\tau_i/\tilde{\mu}_0} \right. \\ &\left. + \tilde{R}(\mu_0) \left( e^{-(2a-\tau_i)/\tilde{\mu}_0} - e^{-(2a-\tau_{i-1})/\tilde{\mu}_0} \right) \right] \quad (53) \end{aligned}$$

where we have used equation (13) to set  $R(\tilde{\mu}_0) = \tilde{R}(\mu_0)$ .

Similarly, in equations (50) and (51), we have

$$\begin{aligned} J(\tau) &= \frac{\mu_0 \left(1 - \tilde{R}(\mu_0)\right)}{1 - \tilde{R}^2(\mu_0) e^{-2a/\tilde{\mu}_0}} \left( e^{-\tau/\tilde{\mu}_0} - \tilde{R}(\mu_0) e^{-(2a-\tau)/\tilde{\mu}_0} \right) \\ &+ \frac{c}{2} \sum_{j=1}^N \phi_{0j} [E_j(\tau) + N_j(\tau)]. \quad (54) \end{aligned}$$

The transmission and reflection coefficients are

$$T_m = \frac{1}{\mu_0} J(a) \quad (55)$$

and

$$R_m = 1 - \frac{1}{\mu_0} J(0). \quad (56)$$

In order to examine the effect of increasing anisotropy of the incident radiation, we use a synthetic function of the Henyey-Greenstein type [13], viz:

$$\psi(\mu) = \frac{A_0}{(1 + g^2 - 2g\mu)^{3/2}}; \quad 0 < \mu < 1 \quad (57)$$

where

$$A_0 = \frac{g^2(1-g)}{1-g+g^2-(1-g)\sqrt{1+g^2}} \quad (58)$$

and  $\psi$  is normalised to  $\int_0^1 d\mu \mu \psi(\mu) = 1$ . For  $g = 0$ ,  $A_0 = 2$ . Then as  $g \rightarrow 1$ , the incident distribution tends to  $\delta(\mu - 1)$ .

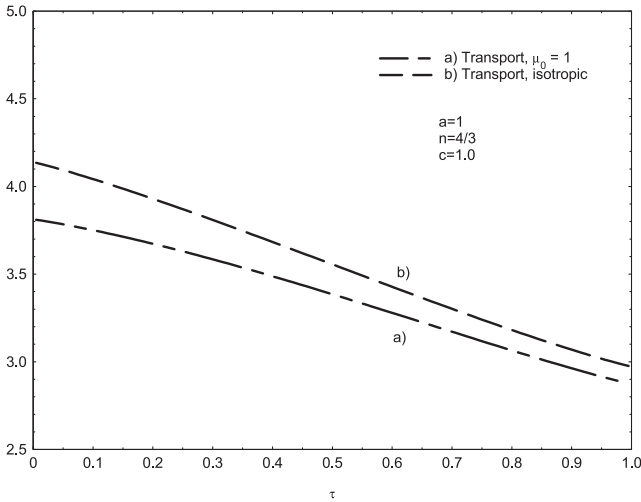


**Fig. 1.** Radiation flux intensity for isotropic and straight-ahead incident source.

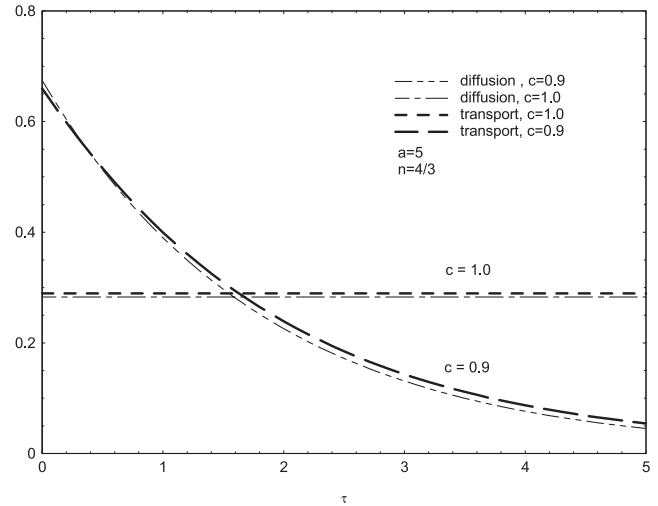


**Fig. 3.** Radiation current for isotropic incident source for transport and diffusion theory.

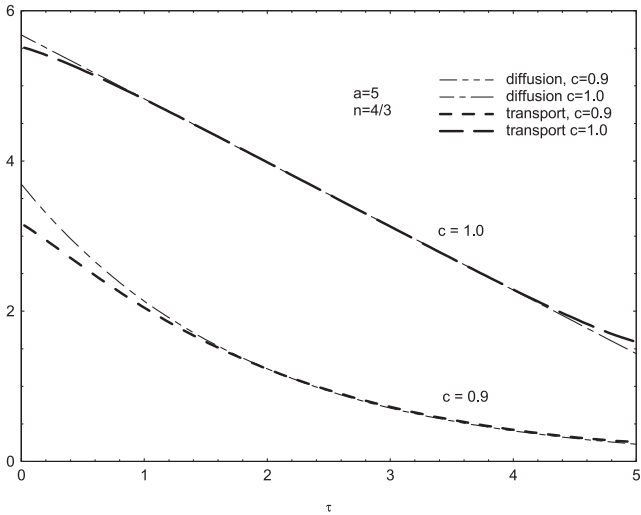


**Fig. 2.** Radiation flux intensity for isotropic incident source for transport and diffusion theory.

### 5.2 Calculations

We have used Fortran and IMSL libraries to evaluate the above sets of equations and associated expressions. This has been done for a variety of parameters and the results are given below. At the outset it is important to note that all the values for  $n = 1$ , i.e. no reflection, agree with the results given by van de Hulst [13] to 4 significant figures. It is the values for  $n > 1$  which are new and are presented as benchmark values. In addition, to check conservation, we note for the case  $c = 1$ , and arbitrary refractive index  $n$ , that  $R+T = 1$ , i.e. there is no absorption. This result is found to hold for up to 8 significant figures in our numerical work and adds confidence to the calculations. In the following we shall give tables and figures of some of the more important parameters of the slab problem which we offer as benchmarks against which to compare other methods. We also give some diffusion theory results. A further test of consistency is obtained by setting  $R_2 = 1$  in equa-

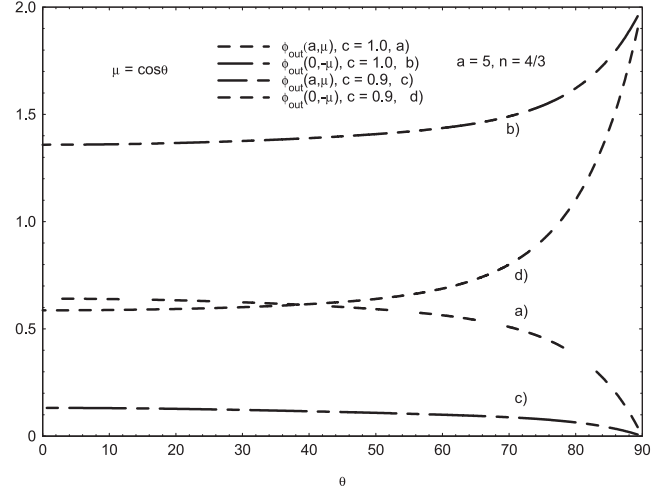


**Fig. 4.** Emergent angular distributions at faces  $\tau = 0$  and  $a$ .

tion (5). That equation then reduces to the symmetrical case for a slab of twice the thickness.

Before giving detailed tables of important parameters, we will show graphically some of the general features of the solution. Thus in Figure 1, we have the radiation scalar intensity  $\phi_0(\tau)$  for the case  $a = 1$ ,  $n = 4/3$ ,  $c = 1$  for the two contrasting cases of a mono-directional beam at  $\tau = 0$  and an isotropic source at  $\tau = 0$ , such that in case a)  $\psi(\mu) = \delta(\mu - 1)$  and in case b)  $\psi(\mu) = 2$ . In both cases  $\int_0^1 d\mu \mu \psi(\mu) = 1$ . In Figure 2, we show two cases for  $a = 5$ ,  $n = 4/3$  and  $c = 0.9$  and  $c = 1.0$ . For comparison purposes, we also include the diffusion result. For  $c = 1$ , diffusion theory gives very reasonable accuracy but for  $c = 0.9$ , there are significant deviations near the boundary at  $\tau = 0$ . Nevertheless, overall, diffusion theory is often a satisfactory approximation. In Figure 3, we have the radiation current  $J(\tau)$  for  $a = 5$ ,  $n = 4/3$  and  $c = 0.9$  and  $c = 1.0$  for diffusion and transport theories. For  $c = 1$ , the current  $J(\tau)$  is independent of  $\tau$  because of conservation. On the other hand, for  $c = 0.9$ , absorption leads to attenuation. In both cases, diffusion theory is reasonable. Finally, in Figure 4 we show the emergent angular

**Table 1.** Reflection and transmission coefficients for  $a = 1$ ,  $c = 1$ , isotropic incident source for a range of refractive indices.

$n$	Transport		Diffusion	
	$R_s$	$T_s$	$R_d$	$T_d$
1.0	0.4466	0.5534	0.4286	0.5714
1.2	0.4069	0.5931	0.4366	0.5634
1.4	0.4133	0.5867	0.4701	0.5299
1.6	0.4285	0.5715	0.5009	0.4991
1.8	0.4466	0.5534	0.5270	0.4730
2.0	0.4655	0.5345	0.5493	0.4507

**Table 2.** Reflection and transmission coefficients for  $a = 1$ ,  $c = 0.9$ , isotropic incident source for a range of refractive indices.

$n$	Transport		Diffusion	
	$R_s$	$T_s$	$R_d$	$T_d$
1.0	0.3527	0.4748	0.3337	0.4885
1.2	0.2952	0.4864	0.3131	0.4480
1.4	0.2818	0.4579	0.3189	0.3841
1.6	0.2794	0.4241	0.3241	0.3259
1.8	0.2827	0.3906	0.3276	0.2761
2.0	0.2895	0.3592	0.3306	0.2340

**Table 3.** Reflection and transmission coefficients for  $a = 5$ ,  $c = 1$ , isotropic incident source for a range of refractive indices.

$n$	Transport		Diffusion	
	$R_s$	$T_s$	$R_d$	$T_d$
1.0	0.7923	0.2077	0.7895	0.2105
1.2	0.7366	0.2634	0.7408	0.2592
1.4	0.7002	0.2998	0.7074	0.2926
1.6	0.6769	0.3231	0.6851	0.3149
1.8	0.6630	0.3370	0.6710	0.3290
2.0	0.6555	0.3445	0.6631	0.3369

**Table 4.** Reflection and transmission coefficients for  $a = 1$ ,  $c = 0.9$ , anisotropic beam with normal incidence,  $\mu_0 = 1$  for a range of refractive indices.

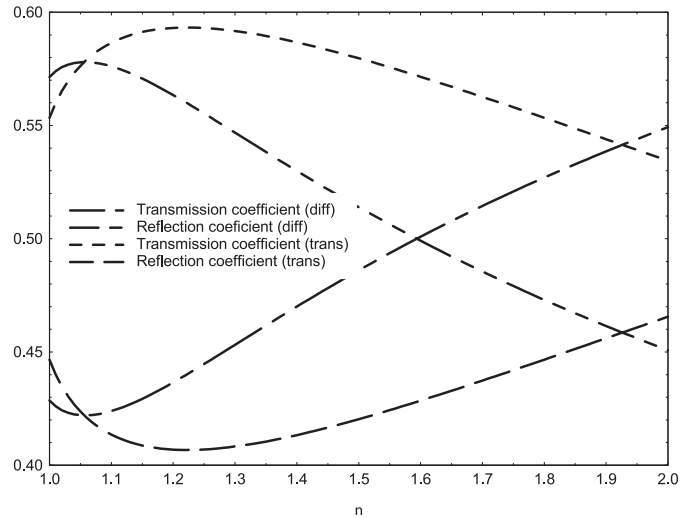
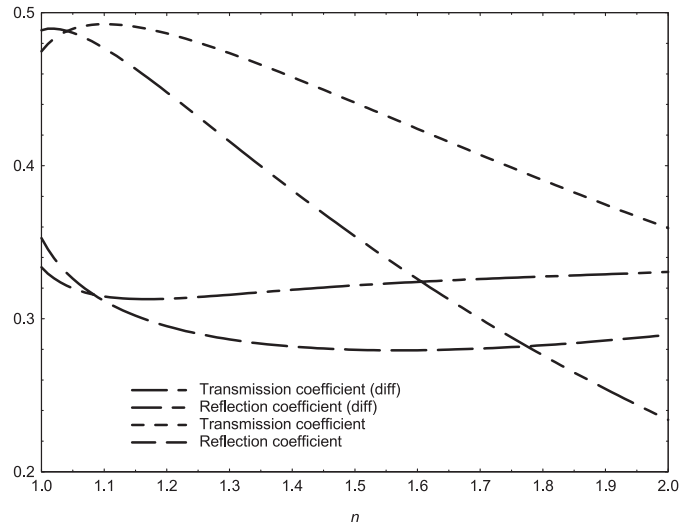
$n$	Transport		Diffusion	
	$R_s$	$T_s$	$R_d$	$T_d$
1.0	0.2674	0.5916	0.3337	0.4885
1.2	0.2343	0.5662	0.2872	0.4649
1.4	0.2231	0.5270	0.2827	0.4044
1.6	0.2230	0.4848	0.2840	0.3452
1.8	0.2297	0.4434	0.2868	0.2928
2.0	0.2409	0.4048	0.2912	0.2478

distributions from the slab faces at  $\tau = 0$  and  $\tau = a$ . This is for  $a = 5$ ,  $n = 4/3$  and  $c = 0.9$  and  $c = 1.0$ .

Tables 1–5 list values of the reflection and transmission coefficients  $R$  and  $T$  for various slab parameters. For comparison, both transport and diffusion theory results are given. To illustrate the results more clearly, Figure 5 shows  $R$  and  $T$  as a function of refractive index  $n$ . An interesting feature is the minimum in  $R$  and maximum in  $T$  at around  $n = 1.2$ . We also note that diffusion theory does

**Table 5.** Reflection and transmission coefficients for  $a = 5$ ,  $c = 0.9$ , anisotropic beam with normal incidence,  $\mu_0 = 1$  for a range of refractive indices.

$n$	Transport		Diffusion	
	$R_s$	$T_s$	$R_d$	$T_d$
1.0	0.4125	0.7665	0.4635	0.5072
1.2	0.3326	0.7159	0.3417	0.5126
1.4	0.2780	0.6282	0.2742	0.4520
1.6	0.2469	0.5351	0.2386	0.3792
1.8	0.2327	0.4498	0.2232	0.3117
2.0	0.2301	0.3766	0.2209	0.2545

**Fig. 5.** Reflection and transmission coefficients  $a = 1$ ,  $c = 1$ , isotropic incidence.**Fig. 6.** Reflection and transmission coefficients  $a = 1$ ,  $c = 0.9$ .

not predict the values very well, which is understandable when it is recognised that  $R$  and  $T$  depend sensitively on the emergent angular distributions; a feature which diffusion (P1) theory does not describe very well. Nevertheless, diffusion theory does predict the maximum and minimum but not in the correct place. Figure 6 repeats the results of Figure 5 but with absorption such that  $c = 0.9$ . In this



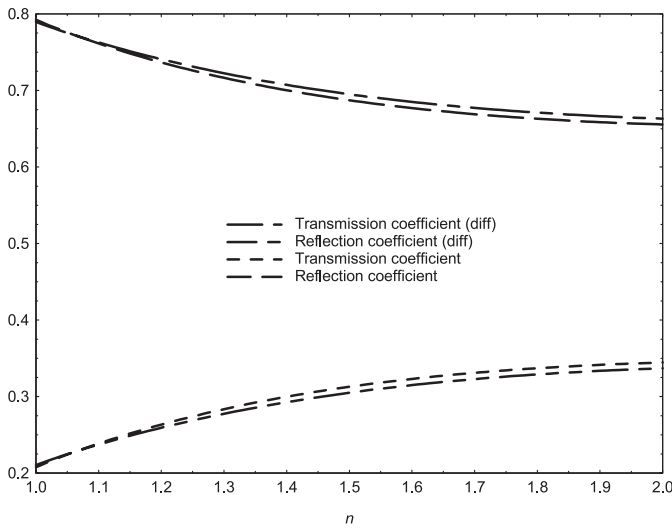


Fig. 7. Reflection and transmission coefficients  $a = 5, c = 1$ .

Table 6. Reflection and transmission coefficients for  $a = 1, c = 1, n = 4/3$ , anisotropic beam with varying angle of incidence  $\cos^{-1} \mu_0$ .

$\mu_0$	Transport		Diffusion	
	$R_s$	$T_s$	$R_d$	$T_d$
0.05	0.8631	0.1369	0.8449	0.1551
0.1	0.7555	0.2445	0.7333	0.2667
0.2	0.6067	0.3933	0.5932	0.4068
0.3	0.5168	0.4832	0.5180	0.4820
0.4	0.4613	0.5387	0.4771	0.5229
0.5	0.4255	0.5745	0.4550	0.5450
0.6	0.4006	0.5994	0.4430	0.5570
0.7	0.3821	0.6179	0.4368	0.5632
0.8	0.3673	0.6327	0.4338	0.5662
0.9	0.3547	0.6453	0.4325	0.5675
1.0	0.3436	0.6564	0.4322	0.5678

case, the maximum for  $T$  is around  $n = 1.1$  and the minimum for  $R$  around  $n = 1.5$ . Finally, we have Figure 7 which is for  $a = 5$  and  $c = 1.0$ . Here there is no maximum or minimum and diffusion theory is a very good approximation. Bearing in mind that diffusion theory becomes better for smaller absorption and slabs that are several mean free paths thick, these results are not unexpected. Table 5 shows  $R$  and  $T$  for an anisotropic beam with normal incidence.

Tables 6 and 7 show the reflection and transmission coefficients for a mono-directional beam for varying values of the incident beam direction  $\vartheta_0 = \cos^{-1} \mu_0$ . Table 6 has  $c = 1$  and Table 7  $c = 0.9$ . Table 8 is presented to show how reflection and transmission coefficients vary as the degree of anisotropy of the incident source goes from isotropic to mono-directional, i.e. as  $g$  goes from zero to unity. Tables 9 and 10 show the emergent angular distributions from the slab faces for a range of values of the refractive index. Table 11 shows the angular distributions for a range of incident angle beam directions.

Table 7. Reflection and transmission coefficients for  $a = 1, c = 0.9, n = 4/3$ , anisotropic beam with varying angle of incidence  $\cos^{-1} \mu_0$ .

$\mu_0$	Transport		Diffusion	
	$R_s$	$T_s$	$R_d$	$T_d$
0.05	0.8160	0.0908	0.8042	0.1161
0.1	0.6783	0.1693	0.6633	0.1996
0.2	0.4962	0.2861	0.4864	0.3045
0.3	0.3914	0.3614	0.3914	0.3609
0.4	0.3298	0.4110	0.3399	0.3914
0.5	0.2925	0.4454	0.3119	0.4080
0.6	0.2688	0.4712	0.2968	0.4169
0.7	0.2529	0.4921	0.2890	0.4216
0.8	0.2414	0.5100	0.2851	0.4239
0.9	0.2326	0.5260	0.2835	0.4248
1.0	0.2253	0.5407	0.2831	0.4251

Table 8. Reflection and transmission coefficients for  $a = 1, c = 0.9, n = 4/3$ , For varying degrees of source anisotropy ([see Eq. (57)].

$g$	Transport		Diffusion	
	$R_s$	$T_s$	$R_d$	$T_d$
0.0	0.2846	0.4686	0.3168	0.4051
0.2	0.2729	0.4802	0.3084	0.4101
0.5	0.2532	0.5017	0.2956	0.4176
0.7	0.2408	0.5173	0.2890	0.4216
0.8	0.2352	0.5252	0.2865	0.4231
0.9	0.2301	0.5330	0.2845	0.4242
0.99	0.2258	0.5399	0.2832	0.4250
1.0	0.2253	0.5407	0.2831	0.4251

## 6 Summary and conclusions

The basic problem of an internally reflective slab irradiated on its surfaces is of some practical importance, as explained in Section 1. We have shown that one can reduce the integro-differential equation for the angular intensity to a single integral equation which incorporates the boundary conditions. Numerical results depend therefore on being able to solve in a practical manner equation (5). For simplicity we have studied the case of a slab irradiated on one side only and with the same reflection coefficients at each surface. To solve this equation requires some deliberation. It is tempting to seek an analytical solution. Unfortunately, with this type of equation no closed form solution is available and the best that can be done is to reduce the problem to a set of coupled Fredholm integral equations. The kernel and source terms of these equations depend, however, on various forms of Chandrasekhar's  $H$ -function [9] and the associated numerical work is fraught with a potential for numerical and algebraic errors. Even the 'half-way house' method using the FN technique [10,11] requires considerable effort. For that reason we have employed a direct numerical assault on the integral equation (5) in which the logarithmic singularity in the kernel, arising from the function  $E_1(|\tau - \tau'|)$  is

**Table 9.** Emergent angular distributions  $\phi_{out}(0, -\mu)$  and  $\phi_{out}(a, \mu)$  from faces 0 and  $a$  for a range of refractive indices.  $a = 1$ ,  $c = 1$ , isotropic incident source.

$n$	1.0		1.2		4/3		1.5		2.0	
$\mu$	$\tau = 0$	$\tau = a$	$\tau = 0$	$\tau = a$	$\tau = 0$	$\tau = a$	$\tau = 0$	$\tau = a$	$\tau = 0$	$\tau = a$
0.0	1.5163	0.4837	2.0000	0.0000	2.0000	0.0000	2.0000	0.0000	2.0000	0.0000
0.1	1.3952	0.6048	1.4687	0.5313	1.5111	0.4889	1.5369	0.4630	1.5508	0.4492
0.2	1.2919	0.7081	1.1781	0.8219	1.2133	0.7867	1.2435	0.7565	1.2808	0.7192
0.3	1.1877	0.8123	1.0167	0.9833	1.0336	0.9664	1.0592	0.9408	1.1157	0.8843
0.4	1.0877	0.9123	0.9201	1.0799	0.9227	1.0773	0.9425	1.0575	1.0125	0.9875
0.5	0.9967	1.0033	0.8553	1.1447	0.8509	1.1491	0.8670	1.1330	0.9467	1.0533
0.6	0.9163	1.0837	0.8067	1.1933	0.8012	1.1988	0.8164	1.1836	0.9041	1.0959
0.7	0.8458	1.1542	0.7667	1.2333	0.7642	1.2358	0.7811	1.2189	0.8761	1.1239
0.8	0.7842	1.2158	0.7319	1.2681	0.7346	1.2654	0.7550	1.2450	0.8576	1.1424
0.9	0.7302	1.2698	0.7006	1.2994	0.7095	1.2905	0.7347	1.2653	0.8453	1.1547
1.0	0.6827	1.3173	0.6719	1.3281	0.6873	1.3127	0.7179	1.2821	0.8369	1.1631

**Table 10.** Emergent angular distributions  $\phi_{out}(0, -\mu)$  and  $\phi_{out}(a, \mu)$  from faces 0 and  $a$  for a range of refractive indices.  $a = 1$ ,  $c = 0.9$ , isotropic incident source.

$n$	1.0		1.2		4/3		1.5		2.0	
$\mu$	$\tau = 0$	$\tau = a$	$\tau = 0$	$\tau = a$	$\tau = 0$	$\tau = a$	$\tau = 0$	$\tau = a$	$\tau = 0$	$\tau = a$
0.0	1.2707	0.3631	2.0000	0.0000	2.0000	0.0000	2.0000	0.0000	2.0000	0.0000
0.1	1.1378	0.4516	1.3162	0.3870	1.3567	0.3386	1.3717	0.3001	1.3429	0.2422
0.2	1.0387	0.5352	0.9645	0.6202	0.9924	0.5721	1.0064	0.5229	0.9907	0.4303
0.3	0.9468	0.6318	0.7794	0.7591	0.7827	0.7229	0.7876	0.6735	0.7862	0.5562
0.4	0.8623	0.7330	0.6761	0.8491	0.6596	0.8219	0.6547	0.7743	0.6627	0.6393
0.5	0.7873	0.8297	0.6131	0.9148	0.5850	0.8908	0.5729	0.8437	0.5868	0.6951
0.6	0.7218	0.9179	0.5702	0.9681	0.5377	0.9424	0.5218	0.8936	0.5400	0.7336
0.7	0.6650	0.9967	0.5379	1.0147	0.5058	0.9841	0.4894	0.9317	0.5115	0.7609
0.8	0.6157	1.0666	0.5115	1.0569	0.4828	1.0199	0.4682	0.9624	0.4948	0.7812
0.9	0.5726	1.1284	0.4888	1.0959	0.4651	1.0519	0.4540	0.9886	0.4858	0.7969
1.0	0.5348	1.1833	0.4686	1.1323	0.4507	1.0814	0.4440	1.0119	0.4818	0.8096

**Table 11.** Emergent angular distributions  $\phi_{out}(0, -\mu)$  and  $\phi_{out}(a, \mu)$  from faces 0 and  $a$  for  $n = 4/3$ ,  $a = 5$ ,  $c = 0.9$ , anisotropic beam source with varying angle of incidence  $\cos^{-1} \mu_0$ .\*

$\mu_0$	0.1		0.2		0.5		0.7		1.0	
$\mu$	$\tau = 0$	$\tau = a$	$\tau = 0$	$\tau = a$	$\tau = 0$	$\tau = a$	$\tau = 0$	$\tau = a$	$\tau = 0$	$\tau = a$
0.1	0.1526	0.1911	0.4630	0.0588	0.1499	0.2099	0.2096	0.3237	0.2844	0.0520
0.2	0.2315	0.2942	0.7025	0.0906	0.2275	0.3230	0.3182	0.4979	0.4321	0.8000
0.3	0.2720	0.3540	0.8254	0.1090	0.2675	0.3886	0.3744	0.5987	0.5087	0.9609
0.4	0.2916	0.3923	0.8852	0.1207	0.2871	0.4303	0.4021	0.6624	0.5471	0.1062
0.5	0.2997	0.4198	0.9100	0.1292	0.2954	0.4600	0.4142	0.7075	0.5643	0.1132
0.6	0.3014	0.4422	0.9152	0.1361	0.2974	0.4840	0.4174	0.7435	0.5697	0.1186
0.7	0.2994	0.4624	0.9093	0.1423	0.2958	0.5053	0.4157	0.7752	0.5683	0.1234
0.8	0.2954	0.4818	0.8971	0.1482	0.2922	0.5257	0.4111	0.8052	0.5630	0.1278
0.9	0.2902	0.5010	0.8815	0.1541	0.2875	0.5458	0.4049	0.8346	0.5555	0.1321
1.0	0.2844	0.5204	0.8641	0.1600	0.2822	0.5658	0.3978	0.8638	0.5468	0.1363
	$\div 10$	$\div 100$	$\div 10$	$\div 10$		$\div 10$		$\div 10$		

\* The last row shows the factor by which the value must be divided

integrated out analytically. This leads to a set of coupled algebraic equations with relatively simple matrix elements and there are simple methods available to solve these equations. One of the disadvantages of such an approach is that it leaves the user with no general idea of the form of the solution. However, as we have seen from equation (20), such a form can be assumed and proves to be consistent with the original integral equation. Only if the singular

integral equations (22) and (23) are solved can we obtain  $A_0$ ,  $B_0$ ,  $A(\omega)$  and  $B(\omega)$ . If only numerical results are required this may not be necessary. For a more fundamental understanding of the solution, then the equation in Section 3 should be solved by the methods outlined above. We have also seen that diffusion theory can be useful under certain circumstances although perhaps not for emergent angular distributions.

$$K_{ij} = K_{ji} = \int_0^1 d\mu \mu R(\mu) \Delta(\mu) \left\{ \begin{array}{l} \left( e^{-\tau_i/\mu} - e^{-\tau_{i-1}/\mu} \right) \left( e^{-\tau_j/\mu} - e^{-\tau_{j-1}/\mu} \right) + \\ e^{-2a/\mu} \left( e^{(\tau_i+\tau_j)/\mu} - e^{(\tau_i+\tau_{j-1})/\mu} - e^{(\tau_{i-1}+\tau_j)/\mu} + e^{(\tau_{i-1}+\tau_{j-1})/\mu} \right) \\ + R(\mu) \left[ \begin{array}{l} e^{(\tau_j-\tau_{i-1})/\mu} - e^{(\tau_{j-1}-\tau_{i-1})/\mu} - e^{(\tau_j-\tau_i)/\mu} + e^{(\tau_{j-1}-\tau_i)/\mu} \\ + e^{(\tau_{i-1}-\tau_j)/\mu} - e^{(\tau_{i-1}-\tau_{j-1})/\mu} - e^{(\tau_i-\tau_j)/\mu} + e^{(\tau_i-\tau_{j-1})/\mu} \end{array} \right] \end{array} \right\}$$

$$N_j(\tau) = \int_0^1 d\mu \mu R(\mu) \Delta(\mu) \left[ \begin{array}{l} e^{-(\tau+\tau_{j-1})/\mu} - e^{-(\tau+\tau_j)/\mu} - e^{-(2a-\tau-\tau_j)/\mu} + e^{-(2a-\tau-\tau_{j-1})/\mu} \\ + R(\mu) \left\{ e^{-(2a+\tau-\tau_j)/\mu} - e^{-(2a+\tau-\tau_{j-1})/\mu} + e^{-(2a-\tau+\tau_j)/\mu} - e^{-(2a-\tau+\tau_{j-1})/\mu} \right\} \end{array} \right]$$

## Appendix A : Matrix elements referred to in the text

$$M_{ij} = E_{ij} + K_{ij}$$

where

$$E_{ii} = 2\Delta\tau - 1 + 2E_3(\Delta\tau)$$

$$E_{ij} = E_3(\tau_i - \tau_{j-1}) - E_3(\tau_i - \tau_j) + E_3(\tau_{i-1} - \tau_j) \\ - E_3(\tau_{i-1} - \tau_{j-1}) ; i > j$$

$$E_{ij} = E_{ji} ; i < j$$

see equation above

$$E_j(\tau) = E_3(\tau - \tau_j) - E_3(\tau - \tau_{j-1}) ; \tau > \tau_j \\ = E_3(\tau_j - \tau) - E_3(\tau_{j-1} - \tau) ; \tau < \tau_{j-1} \\ = E_3(\tau_j - \tau) - E_3(\tau - \tau_{j-1}) ; \tau_{j-1} < \tau < \tau_j$$

see equation above

## References

1. M.M.R. Williams, Eur. Phys. J. B **47**, 291 (2005)
2. Th.M. Nieuwenhuizen, J.M. Luck, Phys. Rev. E **48**, 569 (1993)
3. M.C.W. van Rossum, Th.M. Nieuwenhuizen, Rev. Modern Phys. **71**, 313 (1999)
4. J.M. Luck, Th.M. Nieuwenhuizen, Eur. Phys. J. **B7**, 483 (1999)
5. L. Simonot, Mady Elias, E. Charron, Applied Optics **43**, 2580 (2004)
6. B. Davison, *Neutron Transport Theory* (Oxford University Press, 1957)
7. M. Born, E. Wolf, *Principles of Optics*, 7th edn. (Cambridge University Press, 1999)
8. M.M.R. Williams, J. Quant. Spec. Rad Transfer **98**, 358 (2006)
9. M.M.R. Williams, *Mathematical Methods in Particle Transport Theory* (Butterworth, London, 1971)
10. C.E. Siewert, P. Benoist, Nuclear Science and Engineering **69**, 156 (1979)
11. B.D. Ganapol, Ann. Nuclear Energy **31**, 2017 (2004)
12. R. Aronson, J. Opt. Soc. Am. **12**, 2532 (1995)
13. H.C. van de Hulst, *Multiple Light Scattering*, Vol. I (Academic Press, 1980)
14. V.V. Sobolev, *A Treatise on Radiative Transfer* (Van Nostrand, 1963)
15. R. Courant, D. Hilbert, *Methods of Mathematical Physics* Vol. I (Interscience Publishers, 1953)